
Data Mixing Made Efficient: A Bivariate Scaling Law for Language Model Pretraining

Ce Ge

Alibaba Group
Beijing, China
gece.gc@alibaba-inc.com

Zhijian Ma

Alibaba Group
Beijing, China
zhijian.mzj@alibaba-inc.com

Daoyuan Chen

Alibaba Group
Hangzhou, China
daoyuanchen.cdy@alibaba-inc.com

Yaliang Li*

Alibaba Group
Bellevue, USA
yaliang.li@alibaba-inc.com

Bolin Ding

Alibaba Group
Bellevue, USA
bolin.ding@alibaba-inc.com

Abstract

Large language models exhibit exceptional generalization capabilities, primarily attributed to the utilization of diversely sourced data. However, conventional practices in integrating this diverse data heavily rely on heuristic schemes, lacking theoretical guidance. This research tackles these limitations by investigating strategies based on low-cost proxies for data mixtures, with the aim of streamlining data curation to enhance training efficiency. Specifically, we propose a unified scaling law, termed **BIMIX**, which accurately models the bivariate scaling behaviors of both data quantity and mixing proportions. We conduct systematic experiments and provide empirical evidence for the predictive power and fundamental principles of **BIMIX**. Notably, our findings reveal that entropy-driven training-free data mixtures can achieve comparable or even better performance than more resource-intensive methods. We hope that our quantitative insights can shed light on further judicious research and development in cost-effective language modeling.

1 Introduction

The development of advanced language models (LMs) has become a cornerstone of artificial intelligence [36], revolutionizing capabilities for comprehending and generating human-like text across a broad spectrum of applications and industries [8]. As efforts continue to create more potent LMs, the significance of training data in enhancing model performance and generalizability cannot be overstated [33]. With the proliferation and diversification of datasets, efficiently harnessing this abundance of information is vital for cultivating models that excel across multiple domains, aspiring toward the realization of Artificial General Intelligence [32, 10].

Traditionally, LM development has heavily relied on heuristic presets [17] or iterative refinement [50] for mixing diverse data sources, often entailing sub-optimal performance and resource-intensive search procedures. Nonetheless, the paradigm is recently shifting towards more efficient

*Corresponding author.

methodologies that judiciously consider the trade-off between computational effort and model quality [49, 1, 16, 43]. In this paper, we aim to push the paradigm more principled by deriving actionable insights from a scaling framework [22] and investigating the following research questions:

- (1) **Is it possible to employ low-overhead, proxy-based measures to quantify the importance of data across diverse domains?** If so, what specific type of proxy proves most effective? Can such approaches yield model performance comparable to, or surpassing, that inferred from more resource-intensive data mixing methods?
- (2) **Can we establish a formal, predictive function to describe the relationship between data mixtures and their effects on model training outcomes?** If achievable, what are the critical variables in this function, and how precise can it be? Furthermore, can this principle be applied effectively to larger-scale scenarios?

The key part of our answer is a new scaling law for LM data mixing, termed **BIMIX**, which is motivated by observations on the disentangled scaling behaviors of LMs in terms of *data mixing proportions* and training data quantity (embodied by *model training steps*). The proposed scaling law quantitatively characterizes how these two data-related variables impact the validation loss of the trained models, and provides good interpretability and functional extensibility. Furthermore, we incorporate several entropic proxies to determine the coefficients of **BIMIX** and apply the law to scalable training scenarios in a predictable manner, which enables efficient and robust optimization of data mixing proportions following data diversity cues.

With substantial experiments, we demonstrate that **BIMIX** can be precisely fitted across diverse datasets, and effectively and efficiently used in data mixture optimization, leading to faster convergence and better downstream task performance over strong high-cost baselines. Moreover, we showcase several practical insights of **BIMIX** such as selecting the most promising data mixtures without prior training and harnessing customized constraints to optimize mixing proportions.

Our contributions can be summarized as follows:

- We introduce a new bivariate scaling law, **BIMIX**, from the perspective of LM data, which accurately reveals the predictable impact of data quantity and mixing proportions, and provides theoretical guidance for optimizing LM data mixtures.
- We broaden the use of entropy proxies to language model pretraining, leveraging entropic scores to efficiently fit **BIMIX**. Among four entropy proxies that yield positive improvements, conditional entropy demonstrates the most significant benefit.
- We validate the preciseness and usefulness of **BIMIX** through comprehensive experiments, and explore and discuss several practical implications. Our code is released at *anonymous link* to facilitate insightful research and productive development in language modeling.

2 Related Work

Pretraining Data Mixtures The coverage and diversity of pretraining data play significant roles in shaping the generalization capabilities of language models [38, 7, 45]. Data mixtures from multiple sources, such as the Pile [17] and ROOTS [31], are typically curated based on manually devised rules. However, the heuristics lack universal standards and portability. The GLaM dataset [14] determined domain weights based on the component performance in a small model; however, specific details are not disclosed. SlimPajama-DC [41] investigated the effects of data mixtures using a set of predefined configurations and delivered several insights. Recently, DoReMi [50] and DoGE [15] proposed learning-based methods to optimize domain proportions by iterating between training reference and proxy models. These methods provide viable pathways but require considerable computational costs. In contrast, our study demonstrates that entropy proxies can produce data mixtures of comparable or even superior quality, while providing a more practical training-free solution. Besides, Chen et al. [11] explored the effects of data sequencing from a curriculum learning perspective, whereas our research focuses on the concurrent integration of diverse data domains.

Neural Scaling Laws Investigations into the scaling behavior of neural models have spanned across domains such as computer vision [29, 52, 25, 42] and natural language processing [24, 19, 18, 2]. Kaplan et al. [28] thoroughly evaluated the scalability of Transformer architectures across a wide range of model sizes and data volumes. Chinchilla [22] identified similar scaling patterns through rigorous

experimentation and suggested a slightly different configuration for compute-optimal pretraining. The impactful GPT-4 model [36] validated the predictive accuracy of scaling laws and underscored their important role in the development of large language models. Concurrently, additional research efforts seek to elucidate the principles governing scaling laws [40, 35] and to investigate scaling effects on downstream tasks [44, 23, 9, 12]. In the context of data mixtures, Ye et al. [51] proposed a composite exponential law to capture the interactions among domains; yet, its scalability is challenged by increased complexity for expanding domain numbers, as compared in Appendix C (theoretically) and in Appendix D (empirically). Our study distinguishes itself through two notable aspects: First, an efficiently parameterized scaling law is introduced to accurately model the scaling behavior associated with the internal composition of datasets. Second, the proposed bivariate functional form on *two input variables* enables joint scaling across both dimensions of *data quantity* and *domain proportion*.

3 BIMIX: Compute-Efficient Data Mixing

In this section, we present our bivariate scaling law for data mixing, and disentangle its scaling behaviors across two dimensions. Also, we examine entropy-driven proxies for efficient mixture estimation. Lastly, we provide practical guidance on data mixture optimization for LM pretraining.

3.1 Bivariate Scaling Law

Conventional scaling laws primarily focus on the scaling behavior of model performance with respect to primary input variables such as the number of parameters. In the context of data-centric scaling, especially for language models trained on diverse domains, both the data quantity and domain proportion dimensions emerge as significant factors. We propose a bivariate scaling law, termed **BIMIX**, to jointly model the data scaling behaviors across these two dimensions:

$$\mathcal{L}(s, r) = \left(\frac{\mathcal{A}}{s^\alpha} + \mathcal{C} \right) \frac{\mathcal{B}}{r^\beta}, \quad (1)$$

where the constants \mathcal{A} , \mathcal{B} , \mathcal{C} and exponents α , β are coefficients to fit. The validation loss $\mathcal{L}(s, r)$ on a data domain can be jointly determined by the number of training steps s and the domain proportion r in the training data. Through extensive experiments detailed in Sec. 5, we show that **BIMIX** not only accurately fits observations but also provides extrapolative ability for reliable prediction.

3.2 Disentangling Scaling Behavior

Delving into the details of Equation (1), the scaling law is elegantly constructed in a multiplicative functional form, anticipated to provide enhanced interpretability and flexible extensibility. Herein, we disentangle its scaling behaviors within the two respective dimensions.

Scaling Step with Fixed Proportions The subplots in Figure 1 showcase the changes in per-domain validation losses across training steps. For brevity, the details of experimental setup is deferred in Sec. 4. The points mark the actual observed values, while the dotted lines represent the fitted Equation (1). The intensity of color indicates different domain proportions. In the log-log plot, each curve corresponding to fixed domain proportion exhibits a curvilinear decreasing trend. This is consistent with the theoretical understanding that the loss function of language models has a lower bound [4, 21, 36]. Given a fixed proportion value \mathcal{R} , the multiplier $\frac{\mathcal{B}}{r^\beta}$ in Equation (1) becomes constant and can be absorbed into constants \mathcal{A} and \mathcal{C}^2 , i.e.,

$$\mathcal{L}(s \mid \mathcal{R}) = \frac{\mathcal{A}_{[\mathcal{R}]}}{s^\alpha} + \mathcal{C}_{[\mathcal{R}]}. \quad (2)$$

Furthermore, these variation curves from a broad perspective seem to exhibit a regular patterns, with a translation transformation $f_{\mathcal{A}}(r)$ corresponding to constant \mathcal{A} , and a curvature transformation $f_{\mathcal{C}}(r)$ corresponding to constant \mathcal{C} , both as functions of the number of training steps r , i.e.,

$$\mathcal{L}(s, r) = \frac{f_{\mathcal{A}}(r)}{s^\alpha} + f_{\mathcal{C}}(r). \quad (3)$$

²For detailed explanations of the symbols used, see Appendix A.

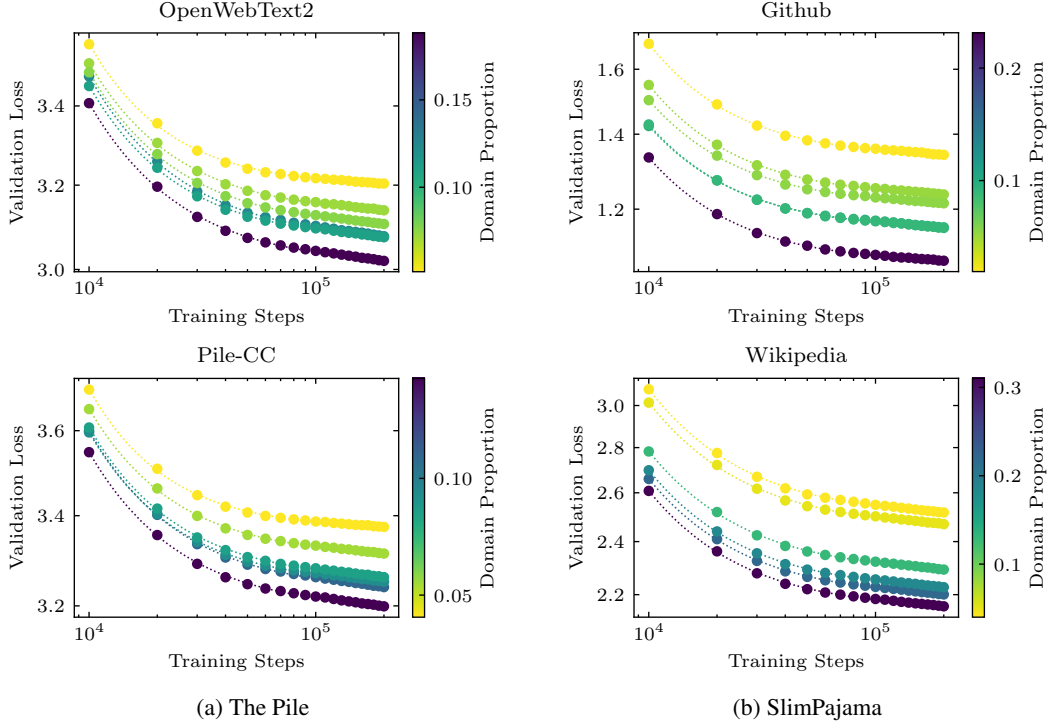


Figure 1: Domain validation loss as a function of training step with different domain proportions.

By positing a shared multiplicative transformation, we can decompose the bivariate loss function into a modulation of an univariate scaling law $\mathcal{L}(s)$ effected by a shared transformation $f(r)$:

$$\mathcal{L}(s, r) \approx \frac{f(r)\mathcal{A}}{s^\alpha} + f(r)\mathcal{C} = f(r)\mathcal{L}(s). \quad (4)$$

Scaling Proportion at Fixed Steps From another perspective, Figure 2 illustrates the changes in validation loss with respect to varying domain proportions. The log-log plot exhibits a pronounced straight lines, which serves as a signature indication of a standard power-law relationship. For each line corresponding to a fixed training step \mathcal{S} , the validation loss demonstrates a power-law decay in the original space with respect to the increasing domain proportion. When exclusively scaling along the proportion dimension, the multiplier $\frac{\mathcal{A}}{s^\alpha} + \mathcal{C}$ can similarly be absorbed into \mathcal{B} , i.e.,

$$\mathcal{L}(r | \mathcal{S}) = \frac{\mathcal{B}_{[\mathcal{S}]}}{r^\beta}. \quad (5)$$

As additive shifts of straight lines in logarithmic space correspond to multiplications in linear space, the loss function is intuitively derived as a multiplicative construct through transformation $g(s)$:

$$\mathcal{L}(s, r) = \frac{g_{\mathcal{B}}(s)}{r^\beta} \approx \frac{g(s)\mathcal{B}}{r^\beta} = g(s)\mathcal{L}(r). \quad (6)$$

This frames a mutual reflection with Equation (4), which naturally informs our multiplicative conceptualization of the **BIMIX** scaling law.

3.3 Entropy-driven Data Mixtures

To determine the coefficients in Equation (1), a series of actual observations is needed to fit the function. The fitting observations can be obtained by conducting a small set of preliminary training on several data mixtures. Rather than random experimentation, we propose using entropy from information theory as a proxy to engineer efficient and robust data mixtures. We have evaluated various entropy measures as presented in Appendix B, among which conditional entropy was identified as the most representative proxy for reflecting the impact of domains within the training set. Specifically,

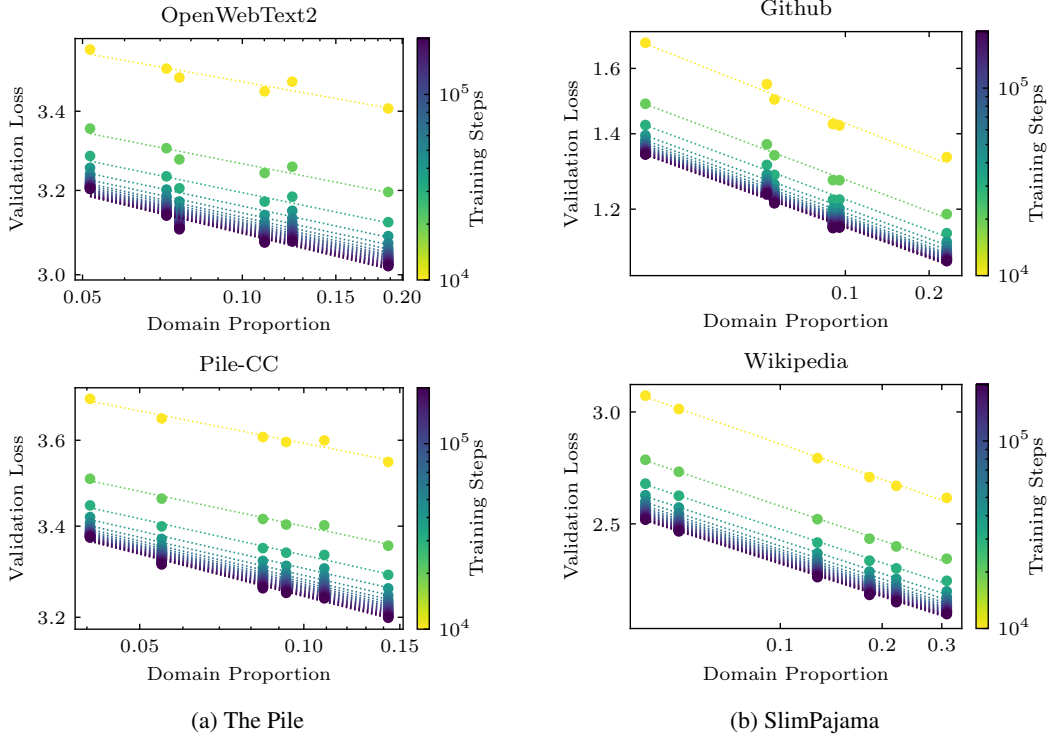


Figure 2: Domain validation loss as a function of domain proportion with different training steps.

given a tokenized dataset $D = \{S_1, S_2, \dots, S_N\}$, where each sample $S_i = (x_1, x_2, \dots, x_T)$ is a token sequence of fixed length T , the conditional entropy (CE) is computed as:

$$\mathcal{H}(X_{t+1}|X_t) = - \sum_{x \in X_t} \sum_{x' \in X_{t+1}} P(x, x') \log P(x' | x), \quad (7)$$

where X_t and X_{t+1} are sets of tokens at positions t and $t + 1$, respectively. The mixing proportions $(\mathcal{R}_1, \mathcal{R}_2, \dots, \mathcal{R}_M)$ of M domains are obtained by exponentially normalizing the entropy measures:

$$\mathcal{R}_i = \frac{e^{\mathcal{H}_i}}{\sum_{j=1}^M e^{\mathcal{H}_j}} = \frac{\mathcal{P}_i}{\sum_{j=1}^M \mathcal{P}_j}, \quad (8)$$

where \mathcal{P}_i denotes the perplexity. The subtlety of this mapping lies in its close connection with the normalized distribution of perplexity [26], which provides a more straightforward interpretation of the expected information gained from learning the domain outcomes. The resulting proportions encourage the domains with higher entropy, which signifies greater diversity, to be learned more extensively. It is noteworthy that the implementation of entropy measurement can be highly efficient, by seamlessly integrated into the tokenization process, incurring negligible computational overhead.

3.4 Practical Strategies for Efficient Data Mixing

The learning efficacy of entropy-driven data mixtures, as illustrated in Sec. 5.1, can rival or surpass that of more compute-intensive methods. Due to its training-free nature, the proxies are well-suited for agile development and model prototyping. For instance, utilizing conditional entropy as an efficient mixing strategy can streamline the initial construction of pretraining dataset and facilitate rapid adjustments of hyperparameters. It is worthwhile to fit **BIMIX** through small-scale experiments before scaling up the target training configuration. This enables extrapolative loss prediction and targeted proportion optimization. The specifics of these practices will be outlined in Sec. 5.3.

4 Experimental Setup

In the experiments, we train models using entropy-driven data mixtures and periodically evaluate the validation loss across various domains. This process yields a series of triplets in the form of $\langle \text{training steps}, \text{domain proportion}, \text{validation loss} \rangle$. We employ the Trust Region Reflective algorithm [6] to fit the coefficients in Equation (1), with results presented in Appendix E.

Datasets Two recognized domain-diverse datasets are used for robust experiments. *The Pile* [17] is a comprehensive language modeling dataset that consists of 22 smaller datasets from different domains. *SlimPajama* [41] consists of 7 sub-datasets from RedPajama [13], with intensive enhancements including NFC normalization, length filtering, and global deduplication. Following [50], the samples are packed in each domain and chunked into sequences of 1024 tokens for training efficiency.

Data Mixtures We consider three types of data mixtures for a comprehensive evaluation: (1) *Baseline* denotes the inherent proportions of datasets, mirroring the natural distribution patterns captured during data collection; (2) *DoReMi* is training-based solution for multi-round mixture optimization; and (3) entropy-driven proxies including Conditional Entropy (*CE*), Shannon Entropy (*SE*), Joint Entropy (*JE*), and Von Neumann Entropy (*VNE*).³

Models We adopt the same transformer architecture as employed in DoReMi [50] for a fair comparison. Specifically, the model comprises 12 Transformer decoders, each featuring an embedding dimension of 768, 12 attention heads, and a $4 \times$ MLP hidden size. The tokenizer is BPE-based GPT-NeoX [5] with a vocabulary size of 50,277. Experiments of 1B models are shown in Appendix D.

Training Details Experiments are conducted under controlled hyperparameters. Each training run undergoes 200,000 update steps with a global batch size of 512. The optimizer is AdamW [34] with $\beta_1 = 0.9$, $\beta_2 = 0.99$, $\epsilon = 1 \times 10^{-8}$, and a weight decay of 0.01. The learning rate, initiated at 1×10^{-3} , decays exponentially by a factor of $10 \times$ throughout the training course. We leverage data parallelism across eight NVIDIA A100 80GB GPUs alongside bfloat16 mixed precision to improve throughput. A single-round DoReMi training takes 670 GPU hours on this infrastructure.

Metrics for Trained Models The models, trained on these above data mixtures, are assessed using a range of one-shot generative downstream tasks as outlined in GPT-3 [7], including TriviaQA [27], NaturalQuestions [30], WebQuestions [3], SQuADv2 [39], and LAMBADA [37]. Additionally, we incorporate perplexity as a supplementary and task-agnostic metric to enhance the consistency and stability of the evaluation.

Metrics for Scaling Law Fitness The fitting quality is quantitatively assessed using two metrics:

- *Coefficient of determination (R^2)* [47] quantifies the extent to which observed outcomes are predictable from the hypothesis, which is computed based on the residual sum of squares SS_{res} and the total sum of squares SS_{tot} :

$$R^2 = 1 - \frac{SS_{\text{res}}}{SS_{\text{tot}}}. \tag{9}$$

- *Pearson Correlation Coefficient (PCC)* [48] measures the strength and direction of a linear relationship, which is essentially a normalized measurement of the covariance:

$$\text{PCC} = \frac{\text{cov}(Y, \hat{Y})}{\sigma_Y \sigma_{\hat{Y}}}. \tag{10}$$

The PCC metric is characterized by its invariance to scaling and shifting, in contrast to the sensitivity of R^2 to minor deviations.

5 Results and Analysis

We first evaluate the performance of models trained on different data mixtures (Sec. 5.1). Based on the observations of entropy-driven mixtures, we fit our scaling law and analyze the goodness of fit and functional form specifications (Sec. 5.2). Finally, we provide practical examples of applying our scaling law (Sec. 5.3).

³We showcase the results of *CE* prominently on the main page, as it yields the most substantial advantages. Other proxies also exhibit benefits over competitors, albeit less prominent. For more details of these proxies, refer to Appendix B.1 (definitions), B.2 (accuracy results), B.3 (perplexity results).

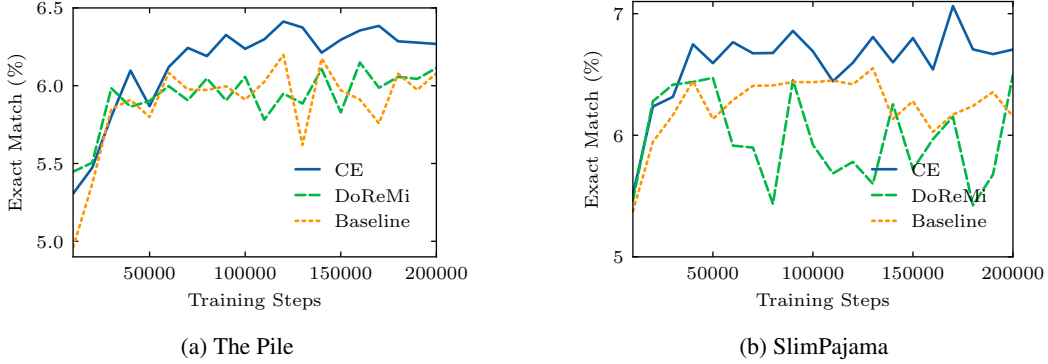


Figure 3: Downstream accuracy of models trained with different data mixtures.

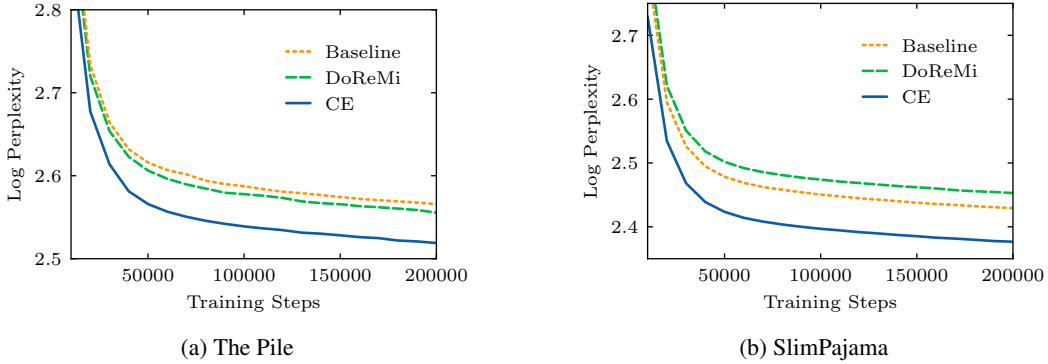


Figure 4: Log-perplexity of models trained with different data mixtures.

5.1 Model Performance across Different Data Mixtures

Downstream Accuracy Figure 3 presents the average exact-match accuracy of models trained on different data mixtures. The CE-driven mixtures are shown to significantly enhance performance across both datasets. The CE method surpasses competitors from the early stages and maintains superiority throughout the training process. For SlimPajama, while both the *Baseline* and *DoReMi* approaches show notable fluctuations, the CE method demonstrates improved stability and more consistent performance. These findings substantiate the notion that entropy proxy is capable of producing highly effective data mixtures while serving as a training-free solution.

Perplexity The evaluation of downstream tasks shows inherently variable and does not consistently capture changes in model efficacy. To address this, we employ perplexity as a statistical and task-agnostic metric that provides a more stable assessment of the models’ generative capacity. As shown in Figure 4, data mixtures informed by CE demonstrate enhanced performance, evidenced by the consistently lower log-perplexity values throughout the training course. This differential performance could be attributable to the closer alignment of the definition of conditional entropy with the model’s training objective of next-token prediction. Nevertheless, these trajectories collectively reveal common patterns that could guide the strategic formulation of effective data mixtures.

5.2 Fitting Analysis of BIMIX

In this section, we analyze the ability of the proposed BIMIX in modeling scaling behaviors and investigate its variant functional forms.

Goodness of Fit The fitness results of Equation (1) when applied to the Pile and SlimPajama datasets is presented in Tables 1 and 2, respectively. A value of 1.0 denotes perfect correlation between the observed and predicted values. In our analysis, both evaluation metrics were computed in logarithmic space to reduce biases. The Pile dataset, encompassing a diverse range of up to 22 components, exhibits impressive R^2 values for most domains, signifying high accuracy of fit. Nonetheless, certain domains such as DM Mathematics, OpenSubtitles, and Wikipedia (en) exhibit

Table 1: Goodness-of-fit on the Pile dataset, including coefficient of determination (R^2) and Pearson correlation coefficient (PCC)

	R^2	PCC		R^2	PCC
ArXiv	0.9781	0.9952	OpenSubtitles	0.8492	0.9995
BookCorpus2	0.9312	0.9982	OpenWebText2	0.9797	0.9995
Books3	0.9930	0.9995	PhilPapers	0.9933	0.9974
DM Mathematics	0.8555	0.9979	Pile-CC	0.9932	0.9995
Enron Emails	0.9935	0.9983	PubMed Abstracts	0.9840	0.9996
EuroParl	0.9824	0.9926	PubMed Central	0.9766	0.9996
FreeLaw	0.9396	0.9994	StackExchange	0.9901	0.9996
Github	0.9938	0.9996	USPTO Backgrounds	0.9572	0.9996
Gutenberg (PG-19)	0.9814	0.9995	Ubuntu IRC	0.9594	0.9897
HackerNews	0.9145	0.9993	Wikipedia (en)	0.8769	0.9995
NIH ExPorter	0.9642	0.9993	YoutubeSubtitles	0.9802	0.9977

Table 2: Goodness-of-fit measures on the SlimPajama dataset

	R^2	PCC
ArXiv	0.9920	0.9997
Books	0.9941	0.9996
C4	0.9856	0.9996
CommonCrawl	0.9957	0.9996
Github	0.9923	0.9996
StackExchange	0.9851	0.9996
Wikipedia	0.9964	0.9996

Table 3: Analysis of different functional forms

\mathcal{C}	\mathcal{D}	\mathcal{E}	The Pile		SlimPajama	
			R^2	PCC	R^2	PCC
			0.7386	0.8829	0.7856	0.8914
		✓	0.8662	0.9712	0.8703	0.9612
	✓		0.7460	0.8829	0.7896	0.8914
	✓	✓	0.8683	0.9713	0.8724	0.9611
✓			0.9570	0.9984	0.9916	0.9996
✓		✓	0.9643	0.9984	0.9919	0.9996
✓	✓		0.9644	0.9984	0.9955	0.9996
✓	✓	✓	0.9686	0.9984	0.9956	0.9996

exceptions, likely due to their unique linguistic structures and inter-domain duplications, which interfere with the effective application of proportions. Despite these outliers, Pearson Correlation Coefficient (PCC) consistently approaches 1.0, indicating robust linear relationships across domains. In comparison, the SlimPajama dataset exhibits uniformly high R^2 and PCC scores in various domains, emphasizing the importance of thorough data cleaning for consistent and robust fitting accuracy.

Functional Form Specification The form of our scaling law in Equation (1) aims to strike a balance between accurately fitting empirical observations and effectively capturing the inherent scaling characteristics. Increasing parameterization can improve the law’s functional complexity to better accommodate data variability; yet, this is accompanied by potential trade-offs in generalizability. Following the discussion, a generalized form of Equation (1) with additional constant terms included can be expressed as follows:

$$\mathcal{L}(s, r) = \left(\frac{\mathcal{A}}{s^\alpha} + \mathcal{C} \right) \left(\frac{\mathcal{B}}{r^\beta} + \mathcal{D} \right) + \mathcal{E}. \quad (11)$$

We conduct comprehensive ablation studies to assess variants of its functional forms, with the comparative results summarized in Table 3. Examination of the numerical results of its first four rows reveals that the introduction of constant \mathcal{E} results in a more pronounced improvement in fitting quality compared to \mathcal{D} , yet their combination yields only incremental improvements. Most importantly, the inclusion of constant \mathcal{C} markedly improves performance and consistently achieves high levels, highlighting its pivotal role in characterizing the scaling behavior. The last three rows of the table show that incorporating constants \mathcal{D} and \mathcal{E} yields only marginal improvements, despite the increased complexity. In light of the analysis, we prefer the simpler form of Equation (1) as the Occam’s razor suggests. Unless specifically required for heightened fitting precision, over-parameterized forms generally need more observational data for reliable estimation and are at higher risk of overfitting.

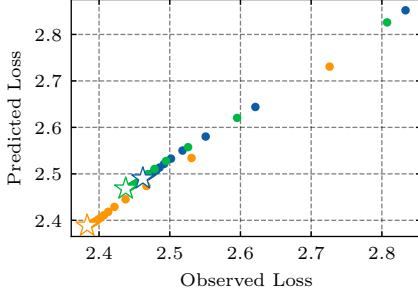


Figure 5: Correlation analysis between observed and predicted validation losses on unseen data mixtures.

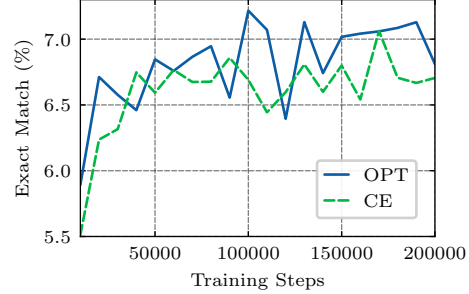


Figure 6: Accuracy comparison on SlimPajama: **BIMIX**-optimized (OPT) versus conditional entropy (CE) driven data mixtures.

5.3 Practical Implications

The proposed scaling law models data scaling across dual dimensions of quantity and proportion, offering broad practical prospects. We present two typical practices to demonstrate its applicability.

Mixture Selection Traditional strategies for creating data mixtures have typically depended on trial-and-error methods, which are both labor-intensive and resource-consuming. The development of our scaling law offers a methodical advance by providing a predictive approach to efficiently assess data mixtures. To evaluate the law’s efficacy, we perform an experimental analysis on a series of new triplet observations from three data mixtures that were not used to fit our scaling law. The analysis involves predicting validation losses using the fitted scaling law and comparing the predictions with the actual observations. As shown in Figure 5, a pronounced linear correlation between the predicted and observed losses is established, confirming the law’s predictive accuracy. Stars in the figure indicate the final validation losses, reflecting the alignment of the predicted mixture rankings with the actual relative performance. These findings underscore the law’s value in streamlining the assessment of unseen mixtures, facilitating informed and training-free data selection prior to extensive training.

Proportion Optimization We further demonstrate the law’s functionality potential to be extended for the direct optimization of mixing proportions with constrained minimization. This method adeptly incorporates practical considerations, such as utilizing intrinsic distribution traits as priors and tailoring domain proportions to the nuanced demands of specific scenarios. A generalized form of the reduced validation loss is the weighted sum over M domains:

$$\bar{\mathcal{L}}(r | \mathcal{S}) = \sum_{i=1}^M w_i \mathcal{L}(r_i | \mathcal{S}), \quad w \in \Delta^{M-1}, \quad (12)$$

where w is a flexible weighting vector within a $(M-1)$ -dimensional simplex. The objective is to minimize the weighted loss subject to the constraint that the sum of domain proportions r equals one:

$$\arg \min_{r \in [0,1]^M} \bar{\mathcal{L}}(r | \mathcal{S}) \quad \text{s.t.} \quad \sum_{i=1}^M r_i = 1. \quad (13)$$

This problem constitutes a classic constrained minimization challenge, solvable through techniques such as Lagrange multipliers and numerical optimization [46]. As shown in Figure 6, the optimized data mixture (OPT)⁴ by our scaling law yields enhanced average performance on downstream tasks compared to the CE method. Nonetheless, the conditional-entropy proxy still demonstrates competitive performance, affirming it as a strong candidate for training-free data mixing method.

6 Conclusion and Discussion

In summary, we present a novel bivariate scaling law that mathematically models the combined impacts of training steps and domain proportion on model performance. Extensive experiments

⁴The mixture recipes are presented in Appendix F.

confirm the preciseness and effectiveness of the law, and demonstrate that entropy-driven data mixtures can achieve good model performance without training overhead. Our work not only provides a systematic and scalable approach for optimizing data mixtures, but also leads to several practical insights into effective-yet-efficient solutions for language model pretraining.

Reflecting on the broader implications, our research advances more economical and environmentally friendly AI development, heralding a shift towards sustainable and universally accessible AI practices. Although marked as effective, the entropic proxies provide only an approximation of the data's intrinsic value and might overlook subtle, domain-specific nuances. Future work aims to extend these insights to multimodal contexts and explore methods for dynamically modulating mixing proportions.

References

- [1] A. Albalak, L. Pan, C. Raffel, and W. Y. Wang. Efficient online data mixing for language model pre-training, 2023, 2312.02406.
- [2] Y. Bansal, B. Ghorbani, A. Garg, B. Zhang, C. Cherry, B. Neyshabur, and O. Firat. Data scaling laws in NMT: The effect of noise and architecture. In *Proceedings of the 39th International Conference on Machine Learning*, volume 162 of *Proceedings of Machine Learning Research*, pages 1466–1482, 17–23 Jul 2022.
- [3] J. Berant, A. Chou, R. Frostig, and P. Liang. Semantic parsing on Freebase from question-answer pairs. In *Proceedings of the 2013 Conference on Empirical Methods in Natural Language Processing*, pages 1533–1544, Oct. 2013.
- [4] C. M. Bishop. Pattern recognition and machine learning. *Springer google schola*, 2:645–678, 2006.
- [5] S. Black, S. Biderman, E. Hallahan, Q. Anthony, L. Gao, L. Golding, H. He, C. Leahy, K. McDonell, J. Phang, M. Pieler, U. S. Prashanth, S. Purohit, L. Reynolds, J. Tow, B. Wang, and S. Weinbach. GPT-NeoX-20B: An open-source autoregressive language model. In *Proceedings of BigScience Episode #5 – Workshop on Challenges & Perspectives in Creating Large Language Models*, pages 95–136, May 2022.
- [6] M. A. Branch, T. F. Coleman, and Y. Li. A subspace, interior, and conjugate gradient method for large-scale bound-constrained minimization problems. *SIAM Journal on Scientific Computing*, 21(1):1–23, 1999.
- [7] T. B. Brown, B. Mann, N. Ryder, M. Subbiah, J. Kaplan, P. Dhariwal, A. Neelakantan, P. Shyam, G. Sastry, A. Askell, S. Agarwal, A. Herbert-Voss, G. Krueger, T. Henighan, R. Child, A. Ramesh, D. M. Ziegler, J. Wu, C. Winter, C. Hesse, M. Chen, E. Sigler, M. Litwin, S. Gray, B. Chess, J. Clark, C. Berner, S. McCandlish, A. Radford, I. Sutskever, and D. Amodei. Language Models are Few-Shot Learners. In *Advances in Neural Information Processing Systems*, volume 33, pages 1877–1901, May 2020, 2005.14165.
- [8] S. Bubeck, V. Chandrasekaran, R. Eldan, J. Gehrke, E. Horvitz, E. Kamar, P. Lee, Y. T. Lee, Y. Li, S. Lundberg, H. Nori, H. Palangi, M. T. Ribeiro, and Y. Zhang. Sparks of artificial general intelligence: Early experiments with gpt-4, 2023, 2303.12712.
- [9] E. Caballero, K. Gupta, I. Rish, and D. Krueger. Broken neural scaling laws. In *The Eleventh International Conference on Learning Representations*, 2023.
- [10] D. Chen, Y. Huang, Z. Ma, H. Chen, X. Pan, C. Ge, D. Gao, Y. Xie, Z. Liu, J. Gao, Y. Li, B. Ding, and J. Zhou. Data-juicer: A one-stop data processing system for large language models. In *Proceedings of the 2024 International Conference on Management of Data*, SIGMOD ’24, 2024.
- [11] M. F. Chen, N. Roberts, K. Bhatia, J. Wang, C. Zhang, F. Sala, and C. Ré. Skill-it! A Data-Driven Skills Framework for Understanding and Training Language Models. In *Advances in Neural Information Processing Systems*, volume 36, pages 36000–36040, July 2023, 2307.14430.
- [12] M. Cherti, R. Beaumont, R. Wightman, M. Wortsman, G. Ilharco, C. Gordon, C. Schuhmann, L. Schmidt, and J. Jitsev. Reproducible scaling laws for contrastive language-image learning. In *Proceedings of the IEEE/CVF Conference on Computer Vision and Pattern Recognition (CVPR)*, pages 2818–2829, June 2023.
- [13] T. Computer. Redpajama: An open source recipe to reproduce llama training dataset, Apr. 2023.
- [14] N. Du, Y. Huang, A. M. Dai, S. Tong, D. Lepikhin, Y. Xu, M. Krikun, Y. Zhou, A. W. Yu, O. Firat, B. Zoph, L. Fedus, M. P. Bosma, Z. Zhou, T. Wang, E. Wang, K. Webster, M. Pellat, K. Robinson, K. Meier-Hellstern, T. Duke, L. Dixon, K. Zhang, Q. Le, Y. Wu, Z. Chen, and C. Cui. GLaM: Efficient Scaling of Language Models with Mixture-of-Experts. In *Proceedings of the 39th International Conference on Machine Learning*, volume 162 of *Proceedings of Machine Learning Research*, pages 5547–5569, 2022.
- [15] S. Fan, M. Pagliardini, and M. Jaggi. DoGE: Domain Reweighting with Generalization Estimation, Oct. 2023, 2310.15393.
- [16] D. Friedman and A. B. Dieng. The vendi score: A diversity evaluation metric for machine learning. *Transactions on Machine Learning Research*, 2023.
- [17] L. Gao, S. Biderman, S. Black, L. Golding, T. Hoppe, C. Foster, J. Phang, H. He, A. Thite, N. Nabeshima, S. Presser, and C. Leahy. The Pile: An 800GB Dataset of Diverse Text for Language Modeling, Dec. 2020, 2101.00027.

- [18] B. Ghorbani, O. Firat, M. Freitag, A. Bapna, M. Krikun, X. Garcia, C. Chelba, and C. Cherry. Scaling laws for neural machine translation. In *International Conference on Learning Representations*, 2022.
- [19] M. A. Gordon, K. Duh, and J. Kaplan. Data and parameter scaling laws for neural machine translation. In *Proceedings of the 2021 Conference on Empirical Methods in Natural Language Processing*, pages 5915–5922, Nov. 2021.
- [20] E. Grave, P. Bojanowski, P. Gupta, A. Joulin, and T. Mikolov. Learning word vectors for 157 languages. In *Proceedings of the International Conference on Language Resources and Evaluation (LREC 2018)*, 2018.
- [21] T. Henighan, J. Kaplan, M. Katz, M. Chen, C. Hesse, J. Jackson, H. Jun, T. B. Brown, P. Dhariwal, S. Gray, C. Hallacy, B. Mann, A. Radford, A. Ramesh, N. Ryder, D. M. Ziegler, J. Schulman, D. Amodei, and S. McCandlish. Scaling laws for autoregressive generative modeling, 2020, 2010.14701.
- [22] J. Hoffmann, S. Borgeaud, A. Mensch, E. Buchatskaya, T. Cai, E. Rutherford, D. d. L. Casas, L. A. Hendricks, J. Welbl, A. Clark, T. Hennigan, E. Noland, K. Millican, G. van den Driessche, B. Damoc, A. Guy, S. Osindero, K. Simonyan, E. Elsen, J. W. Rae, O. Vinyals, and L. Sifre. Training Compute-Optimal Large Language Models. In *Advances in Neural Information Processing Systems*, volume 35, Mar. 2022, 2203.15556.
- [23] B. Isik, N. Ponomareva, H. Hazimeh, D. Pappas, S. Vassilvitskii, and S. Koyejo. Scaling laws for downstream task performance of large language models, 2024, 2402.04177.
- [24] M. Ivgi, Y. Carmon, and J. Berant. Scaling laws under the microscope: Predicting transformer performance from small scale experiments. In *Findings of the Association for Computational Linguistics: EMNLP 2022*, pages 7354–7371, Dec. 2022.
- [25] A. Jain, G. Swaminathan, P. Favaro, H. Yang, A. Ravichandran, H. Harutyunyan, A. Achille, O. Dabeer, B. Schiele, A. Swaminathan, and S. Soatto. A meta-learning approach to predicting performance and data requirements. In *Proceedings of the IEEE/CVF Conference on Computer Vision and Pattern Recognition (CVPR)*, pages 3623–3632, June 2023.
- [26] F. Jelinek, R. L. Mercer, L. R. Bahl, and J. K. Baker. Perplexity—a measure of the difficulty of speech recognition tasks. *The Journal of the Acoustical Society of America*, 62(S1):S63–S63, Dec. 1977.
- [27] M. Joshi, E. Choi, D. Weld, and L. Zettlemoyer. TriviaQA: A large scale distantly supervised challenge dataset for reading comprehension. In *Proceedings of the 55th Annual Meeting of the Association for Computational Linguistics (Volume 1: Long Papers)*, pages 1601–1611, July 2017.
- [28] J. Kaplan, S. McCandlish, T. Henighan, T. B. Brown, B. Chess, R. Child, S. Gray, A. Radford, J. Wu, and D. Amodei. Scaling laws for neural language models, 2020, 2001.08361.
- [29] T. Klug and R. Heckel. Scaling laws for deep learning based image reconstruction. In *The Eleventh International Conference on Learning Representations*, 2023.
- [30] T. Kwiatkowski, J. Palomaki, O. Redfield, M. Collins, A. Parikh, C. Alberti, D. Epstein, I. Polosukhin, J. Devlin, K. Lee, K. Toutanova, L. Jones, M. Kelcey, M.-W. Chang, A. M. Dai, J. Uszkoreit, Q. Le, and S. Petrov. Natural questions: A benchmark for question answering research. *Transactions of the Association for Computational Linguistics*, 7:452–466, 2019.
- [31] H. Laurençon, L. Saulnier, T. Wang, C. Akiki, A. V. del Moral, T. L. Scao, L. V. Werra, C. Mou, E. G. Ponferrada, H. Nguyen, J. Froberg, M. Šaško, Q. Lhoest, A. McMillan-Major, G. Dupont, S. Biderman, A. Rogers, L. B. allal, F. D. Toni, G. Pistilli, O. Nguyen, S. Nikpoor, M. Masoud, P. Colombo, J. de la Rosa, P. Villegas, T. Thrush, S. Longpre, S. Nagel, L. Weber, M. R. Muñoz, J. Zhu, D. V. Strien, Z. Alyafeai, K. Almubarak, V. M. Chien, I. Gonzalez-Dios, A. Soroa, K. Lo, M. Dey, P. O. Suarez, A. Gokaslan, S. Bose, D. I. Adelani, L. Phan, H. Tran, I. Yu, S. Pai, J. Chim, V. Lepercq, S. Ilic, M. Mitchell, S. Luccioni, and Y. Jernite. The bigscience ROOTS corpus: A 1.6TB composite multilingual dataset. In *Thirty-sixth Conference on Neural Information Processing Systems Datasets and Benchmarks Track*, 2022.
- [32] A. Lee, B. Miranda, S. Sundar, and S. Koyejo. Beyond scale: the diversity coefficient as a data quality metric demonstrates llms are pre-trained on formally diverse data, 2023, 2306.13840.
- [33] S. Longpre, G. Yauney, E. Reif, K. Lee, A. Roberts, B. Zoph, D. Zhou, J. Wei, K. Robinson, D. Mimno, and D. Ippolito. A pretrainer’s guide to training data: Measuring the effects of data age, domain coverage, quality, & toxicity, 2023, 2305.13169.
- [34] I. Loshchilov and F. Hutter. Decoupled weight decay regularization. In *International Conference on Learning Representations*, 2019.

- [35] E. Michaud, Z. Liu, U. Girit, and M. Tegmark. The quantization model of neural scaling. In *Advances in Neural Information Processing Systems*, volume 36, pages 28699–28722, 2023.
- [36] OpenAI, J. Achiam, S. Adler, S. Agarwal, L. Ahmad, I. Akkaya, F. L. Aleman, D. Almeida, J. Altenschmidt, S. Altman, S. Anadkat, and Others. Gpt-4 technical report, 2024, 2303.08774.
- [37] D. Paperno, G. Kruszewski, A. Lazaridou, N. Q. Pham, R. Bernardi, S. Pezzelle, M. Baroni, G. Boleda, and R. Fernández. The LAMBADA dataset: Word prediction requiring a broad discourse context. In *Proceedings of the 54th Annual Meeting of the Association for Computational Linguistics (Volume 1: Long Papers)*, pages 1525–1534, Aug. 2016.
- [38] A. Radford, J. Wu, R. Child, D. Luan, D. Amodei, and I. Sutskever. Language models are unsupervised multitask learners. *OpenAI Blog*, 1(8):9, 2019.
- [39] P. Rajpurkar, R. Jia, and P. Liang. Know what you don’t know: Unanswerable questions for SQuAD. In *Proceedings of the 56th Annual Meeting of the Association for Computational Linguistics (Volume 2: Short Papers)*, pages 784–789, July 2018.
- [40] U. Sharma and J. Kaplan. Scaling laws from the data manifold dimension. *Journal of Machine Learning Research*, 23(9):1–34, 2022.
- [41] Z. Shen, T. Tao, L. Ma, W. Neiswanger, Z. Liu, H. Wang, B. Tan, J. Hestness, N. Vassilieva, D. Soboleva, and E. Xing. SlimPajama-DC: Understanding Data Combinations for LLM Training, Sept. 2023, 2309.10818.
- [42] B. Sorscher, R. Geirhos, S. Shekhar, S. Ganguli, and A. S. Morcos. Beyond neural scaling laws: beating power law scaling via data pruning. In *Advances in Neural Information Processing Systems*, 2022.
- [43] Z. Sun, C. Ge, J. Wang, M. Lin, H. Chen, H. Li, and X. Sun. Entropy-Driven Mixed-Precision Quantization for Deep Network Design. In *Advances in Neural Information Processing Systems*, volume 35, pages 21508–21520, 2022.
- [44] Y. Tay, M. Dehghani, J. Rao, W. Fedus, S. Abnar, H. W. Chung, S. Narang, D. Yogatama, A. Vaswani, and D. Metzler. Scale efficiently: Insights from pretraining and finetuning transformers. In *International Conference on Learning Representations*, 2022.
- [45] H. Touvron, T. Lavril, G. Izacard, X. Martinet, M.-A. Lachaux, T. Lacroix, B. Rozière, N. Goyal, E. Hambro, F. Azhar, A. Rodriguez, A. Joulin, E. Grave, and G. Lample. LLaMA: Open and Efficient Foundation Language Models. *CoRR*, abs/2302.1, Feb. 2023, 2302.13971.
- [46] P. Virtanen, R. Gommers, T. E. Oliphant, M. Haberland, T. Reddy, D. Cournapeau, E. Burovski, P. Peterson, W. Weckesser, J. Bright, S. J. van der Walt, M. Brett, J. Wilson, K. J. Millman, N. Mayorov, A. R. J. Nelson, E. Jones, R. Kern, E. Larson, C. J. Carey, Í. Polat, Y. Feng, E. W. Moore, J. VanderPlas, D. Laxalde, J. Perktold, R. Cimrman, I. Henriksen, E. A. Quintero, C. R. Harris, A. M. Archibald, A. H. Ribeiro, F. Pedregosa, P. van Mulbregt, and SciPy 1.0 Contributors. SciPy 1.0: Fundamental Algorithms for Scientific Computing in Python. *Nature Methods*, 17:261–272, 2020.
- [47] Wikipedia contributors. Coefficient of determination — Wikipedia, the free encyclopedia. https://en.wikipedia.org/w/index.php?title=Coefficient_of_determination&oldid=1219795749, 2024. [Online; accessed 9-May-2024].
- [48] Wikipedia contributors. Pearson correlation coefficient — Wikipedia, the free encyclopedia. https://en.wikipedia.org/w/index.php?title=Pearson_correlation_coefficient&oldid=1220413504, 2024. [Online; accessed 9-May-2024].
- [49] M. Xia, T. Gao, Z. Zeng, and D. Chen. Sheared LLaMA: Accelerating language model pre-training via structured pruning. In *The Twelfth International Conference on Learning Representations*, 2024.
- [50] S. M. Xie, H. Pham, X. Dong, N. Du, H. Liu, Y. Lu, P. Liang, Q. V. Le, T. Ma, and A. W. Yu. DoReMi: Optimizing Data Mixtures Speeds Up Language Model Pretraining. In *Advances in Neural Information Processing Systems*, volume 36, pages 69798–69818, May 2023, 2305.10429.
- [51] J. Ye, P. Liu, T. Sun, Y. Zhou, J. Zhan, and X. Qiu. Data mixing laws: Optimizing data mixtures by predicting language modeling performance, 2024, 2403.16952.
- [52] X. Zhai, A. Kolesnikov, N. Houlsby, and L. Beyer. Scaling vision transformers. In *Proceedings of the IEEE/CVF Conference on Computer Vision and Pattern Recognition (CVPR)*, pages 12104–12113, June 2022.

A List of Symbols

Table 4: General symbols used in the paper

Symbol	Meaning/Description
r	proportion of a domain in the training data
s	number of training steps
\mathcal{R}	specific value corresponding to r
\mathcal{S}	specific value corresponding to s
α, β	power exponents
$\mathcal{A}, \mathcal{B}, \mathcal{C}, \mathcal{D}, \mathcal{E}$	constant coefficients
$\mathcal{A}_{[\mathcal{R}]}, \mathcal{C}_{[\mathcal{R}]}, \mathcal{B}_{[\mathcal{S}]}$	constant coefficients for conditions defined by \mathcal{R} and \mathcal{S}
D	dataset of a specific domain
M	number of domains
N	number of sequences
ρ	density matrix
λ_i	eigenvalues indexed by i
S_i	token sequence indexed by i
X_t, X_{t+1}	token sets at consecutive positions t and $t + 1$, respectively
x, \tilde{x}	tokens from distinct sets
\mathcal{H}_i	entropy of the domain indexed by i
\mathcal{P}_i	perplexity of the domain indexed by i
Y	observed values
\hat{Y}	predicted values
\bar{Y}	mean of the observed values
$\sigma_Y, \sigma_{\hat{Y}}$	standard deviations
SS_{res}	residual sum of squares, $\sum(Y - \hat{Y})^2$
SS_{tot}	total sum of squares, $\sum(Y - \bar{Y})^2$

Table 5: Functional symbols used in the paper

Symbol	Meaning/Description
$\mathcal{L}(s, r)$	validation loss as a function of variables s and r
$\mathcal{L}(s \mid \mathcal{R})$	validation loss as a function of variable s given specific value \mathcal{R}
$\mathcal{L}(r \mid \mathcal{S})$	validation loss as a function of variable r given specific value \mathcal{S}
$\mathcal{L}(s)$	validation loss as a function of variable s
$\mathcal{L}(r)$	validation loss as a function of variable r
$f_{\mathcal{A}}(r)$	function transforming variable r associated with constant \mathcal{A}
$f_{\mathcal{C}}(r)$	function transforming variable r associated with constant \mathcal{C}
$f(r)$	general function for transforming variable r
$g_{\mathcal{B}}(s)$	function transforming variable s associated with constant \mathcal{B}
$g(s)$	general function for transforming variable s
$P(x, \tilde{x})$	joint probability mass function of tokens x and \tilde{x}
$P(\tilde{x} \mid x)$	conditional probability mass function of token \tilde{x} given token x
$\mathcal{H}(D)$	Shannon entropy of dataset D
$\mathcal{H}(X_t, X_{t+1})$	joint entropy of consecutive tokens
$\mathcal{H}(X_{t+1} \mid X_t)$	conditional entropy of consecutive tokens
$\mathcal{H}(\rho)$	von Neumann entropy of density matrix ρ
$k(S_i, S_j)$	kernel function assessing similarity between sequences S_i and S_j

B Additional Mixture Experiments

B.1 Entropic Proxies

Given a text dataset such as Pile and SlimPajama, we concatenate all samples within each domain and tokenize them into fixed-length sequences of 1024 tokens. During tokenization, we concurrently record the occurrence frequencies of all unigrams and bigrams, in preparation for computing Shannon entropy, joint entropy, and conditional entropy. The process for von Neumann entropy deviates slightly; we employ the FastText [20] model to embed each sample into a 300-dimensional vector, which is utilized to calculate the pairwise similarities within each domain.

Given a tokenized dataset $D = \{S_1, S_2, \dots, S_n\}$, where each sequence $S_i = (x_1, x_2, \dots, x_T)$ is a token sequence of fixed-length T , the following entropic proxies are computed.

Shannon Entropy (SE) $\mathcal{H}(D) = -\sum_{x \in X} P(x) \log P(x)$, where X is the set of all available tokens in the dataset and $P(x)$ denotes the probability of observing token x . This proxy quantifies the expected information content associated with token appearances in the dataset, indicative of the corpus diversity.

Joint Entropy (JE) $\mathcal{H}(X_t, X_{t+1}) = -\sum_{x \in X_t} \sum_{\tilde{x} \in X_{t+1}} P(x, \tilde{x}) \log P(x, \tilde{x})$, where X_t and X_{t+1} represent the sets of tokens at positions t and $t + 1$ across all sequences, respectively. The joint probability mass function $P(x, \tilde{x})$ denotes the actual statistical probability of observing a token x at position t , followed by a token \tilde{x} at position $t + 1$. This measures the average uncertainty associated with consecutive token pairs and highlights the sequential dependencies in the dataset.

Conditional Entropy (CE) $\mathcal{H}(X_{t+1} | X_t) = -\sum_{x \in X_t} \sum_{\tilde{x} \in X_{t+1}} P(x, \tilde{x}) \log P(\tilde{x} | x)$, with X_t , X_{t+1} , and $P(x, \tilde{x})$ as previously defined. The term $P(\tilde{x} | x)$ denotes the conditional probability of observing a token \tilde{x} at position $t + 1$ given the presence of token x at position t . This measures the anticipated level of surprise when predicting the next token in a sequence, providing a clearer understanding of the text’s predictability and its complex linguistic structure.

Von Neumann Entropy (VNE) In physics, the von Neumann entropy is an extension of the concept of Gibbs entropy from classical statistical mechanics to quantum statistical mechanics. For a quantum-mechanical system described by a density matrix ρ , the von Neumann entropy is defined as $\mathcal{H}(\rho) = -\text{Tr}(\rho \log \rho)$, where Tr denotes the trace operation, and \log the matrix logarithm. Recent research has highlighted its utility in quantifying the diversity of datasets from a systems perspective [16]. In the context of data mixture, we define ρ as $K/n \in \mathbb{R}^{n \times n}$, with $K_{ij} = k(S_i, S_j)$ and $k(S_i, S_i) = 1$ for $1 \leq i, j \leq n$, employing a positive semi-definite kernel $k : D \times D \rightarrow \mathbb{R}$. In practice, calculating von Neumann entropy involves deriving the eigenvalues of the density matrix ρ and computing $\mathcal{H}(\rho) = -\sum_{i=1}^N \lambda_i \log \lambda_i$, where the eigenvalues λ_i represent the probability distributions akin to quantum states in text embeddings.

B.2 Downstream Accuracy

Figure 7 illustrates the downstream accuracy of models trained with entropy-driven data mixtures on the Pile dataset. It is observed that Shannon Entropy (SE) and Joint Entropy (JE) both underperform relative to competing methods and display significant volatility during training. In contrast, Conditional Entropy (CE) and Von Neumann Entropy (VNE), achieve superior performance with consistent growth trends. These patterns are echoed in Figure 8, which showcases results from analogous experiments on the SlimPajama dataset; Shannon Entropy and Joint Entropy lead to more erratic performance, while Conditional Entropy and Von Neumann Entropy maintain superior and stable progressions.

Nonetheless, the notable effort required for calculating Von Neumann Entropy—owing to the necessity of text embeddings and pairwise similarity assessments across the dataset—renders its use less efficient. Consequently, Conditional Entropy is favored for its comparable performance benefits and minimal computational overhead.

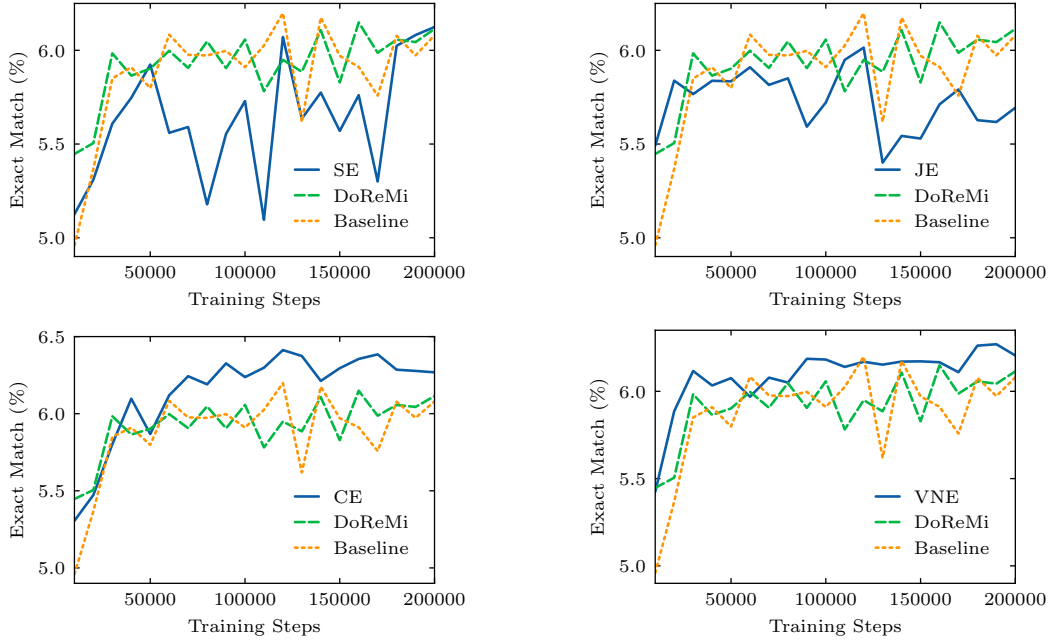


Figure 7: Downstream accuracy of models trained with entropy-driven data mixtures on the Pile dataset.

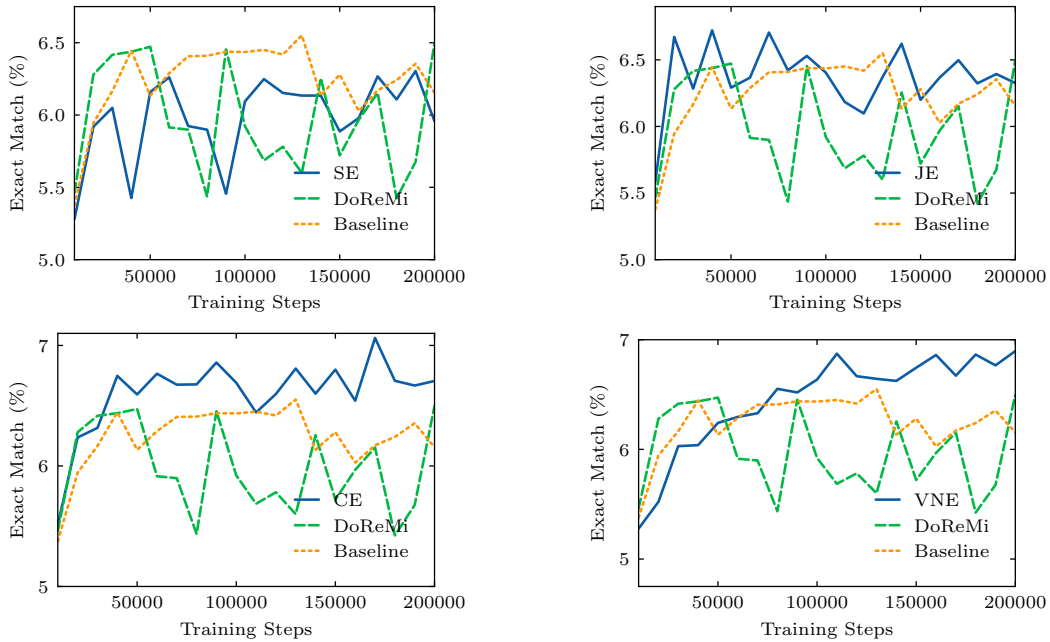


Figure 8: Downstream accuracy of models trained with entropy-driven data mixtures on the SlimPajama dataset.

B.3 Perplexity Evaluation

Figures 9 and 10 show the logarithmic perplexity of models trained with entropy-driven data mixtures on the Pile and SlimPajama datasets, respectively.

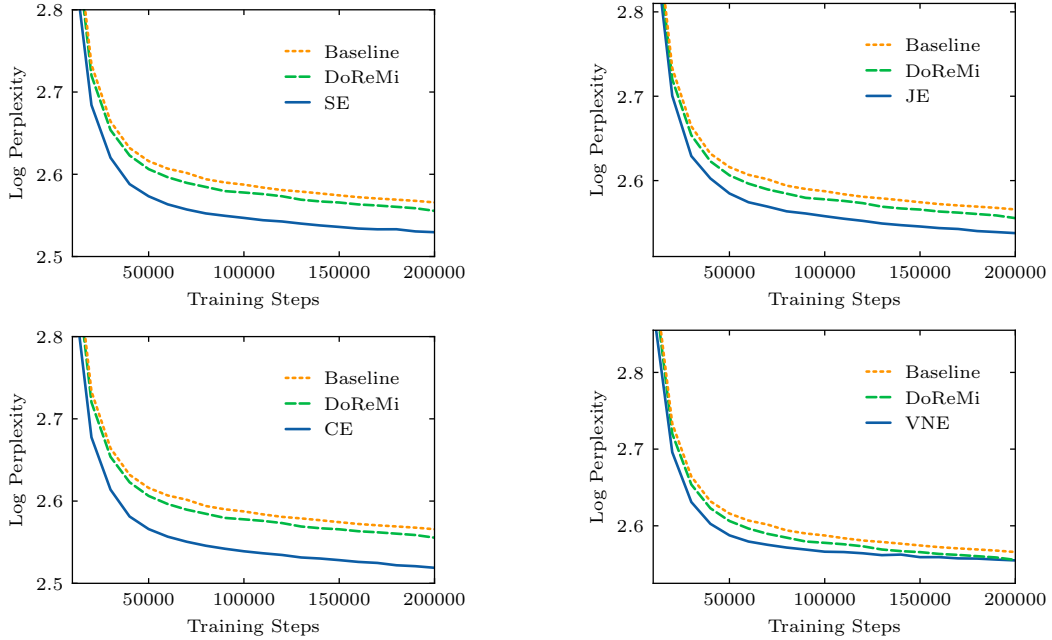


Figure 9: Log-perplexity of models trained with entropy-driven data mixtures on the Pile dataset.

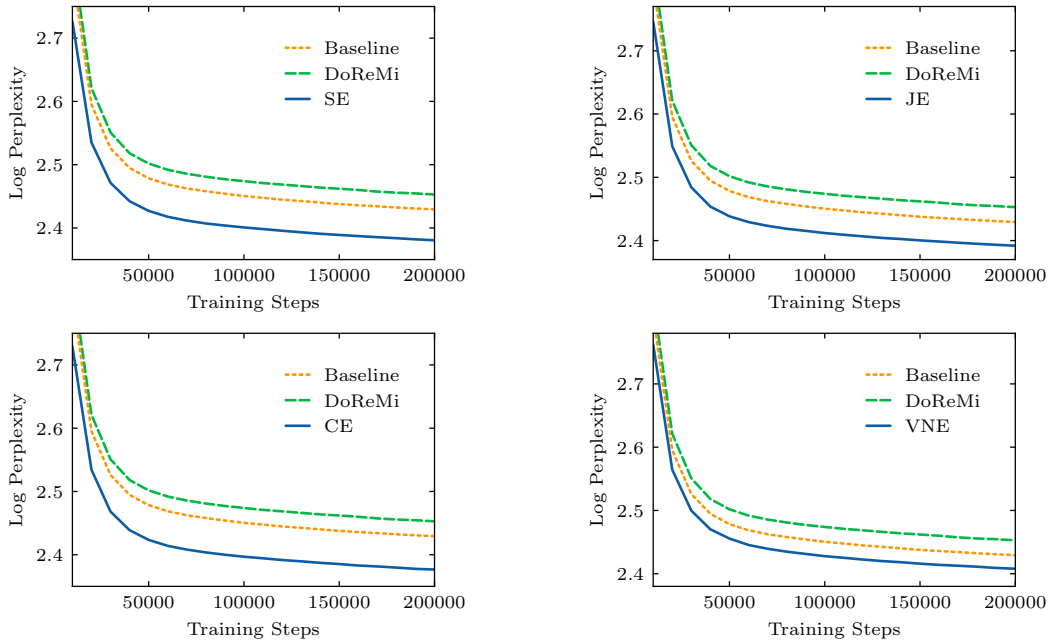


Figure 10: Log-perplexity of models trained with entropy-driven data mixtures on the SlimPajama dataset.

In comparison with alternative approaches, these entropy-driven mixtures effectively reduce the model’s perplexity, implying enhanced certainty in predicting the next token. Notably, among the evaluated proxies, Conditional Entropy achieves the most pronounced reduction in perplexity.

C Complexity Analysis

Table 6: Complexity analysis of mixing laws

Mixing Law	Number of Fitting Coefficients		
	per domain	M domains	M domains, N targets
[51]: $\mathcal{L}(r_{1\dots M}) = c + k \exp(\sum_{j=1}^M t_j r_j)$	$M + 2$	$M^2 + 2M$	$M^2 N + 2MN$
BiMix : $\mathcal{L}(s, r_i) = \left(\frac{A}{s^\alpha} + C\right) \frac{B}{r_i^\beta}$	2	$2M$	$5M$

As presented in Table 6, we evaluate the fitting complexity of our proposed **BiMix** in comparison to the concurrent work, Ye et al.’s composite exponential law [51]. Both equations are showcased to model the validation loss for a single domain. It is crucial to note that the exponential law, denoted as $\mathcal{L}(r_{1\dots M})$, functions based on the proportions (r_1, r_2, \dots, r_M) across all M domains, with no consideration for the number of training steps s . In contrast, our mixing law $\mathcal{L}(s, r_i)$ integrates both the number of training steps s and the mixing proportion r_i of the target domain. We analyze the complexity involved in fitting these two mixing laws across three scenarios, from simple to complex.

Base Case: Fitting an Individual Domain To compute the validation loss for an individual domain, $\mathcal{L}_i(r_{1\dots M})$ aggregates the proportions r_j across all M domains using M weighting coefficients t_{ij} and conducts an affine transformation on the exponential result, requiring one scaling coefficient k_i and one translation coefficient c_i . Altogether, this necessitates $M + 2$ fitting coefficients. Regarding our bivariate mixing law, recall that when the number of training steps is fixed (Sec. 3.2), the term $\frac{A}{s^\alpha} + C$ holds constant and can be absorbed into constant B . Consequently, the mixing law simplifies to Equation (5), which depends solely on two fitting coefficients: a constant $B_{[s]}$ and an exponent β .

General Case: Fitting All Domains Extending from the calculation for an individual domain, the composite requirement for fitting coefficients when addressing all M domains is scaled by a factor of M . In this broader context, the coefficient count required by our mixing law is an order of magnitude smaller compared to that of the composite exponential law.

Extensive Case: Fitting Across Multiple Targets It is important to note that the exponential law does not factor in the variable s , thereby modeling the validation loss at a fixed number of training steps. Upon extending to accommodate multiple training step targets, the exponential law necessitates refitting additional sets of independent coefficients, resulting in a total of $(M^2 + 2M)N$ fitting coefficients. In contrast, our bivariate mixing law accounts for both the number of training steps and domain proportions, enabling the use of shared fitting coefficients across different numbers of training steps. Specifically, only 5 coefficients are required to fit for an individual domain across various training steps; this number scales linearly to $5M$ when generalized to all M domains.

Overall, our bivariate scaling law necessitates significantly fewer coefficients—by an order of magnitude—compared to the composite exponential law, indicating a proportional reduction in the number of required observations for effective fitting. Practically, it is feasible to fit our scaling law with data from just a few (potentially as few as two) sample mixtures. In contrast, the exponential law requires data from a considerably greater pool of sample mixtures—often numbering tens—to ensure sufficient empirical observations. Notably, the high computational efficiency of our method translates into economic and environmental benefits due to reduced resource utilization. Moreover, this resource conservation is achieved without sacrificing model efficacy; instead, it yields better data mixtures and enhanced model performance, as substantiated in Appendix D.

D Results of 1B Models

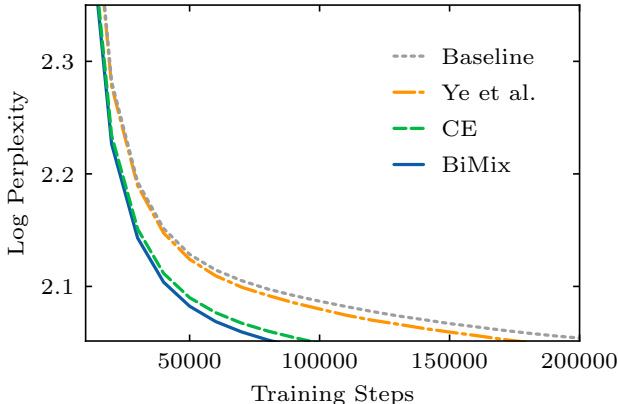


Figure 11: Log-perplexity of 1B models trained with different data mixtures on SlimPajama.

We conducted further experiments, scaling the model architecture to one billion (1B) parameters, and involved the optimal data mixture identified by Ye et al. [51] for comparison. It is noteworthy that the mixing law of Ye et al. encounters scalability challenges when applied to the more diverse, 22-domain Pile dataset. Therefore, our experiments were confined to the 7-domain SlimPajama dataset.

Upon analyzing the data presented in Figure 11, we derive several key findings:

- Every optimized data mixture—including those derived from scaling laws of our **BIMIX** and Ye et al., as well as driven by the conditional entropy proxy—resulted in accelerated model convergence compared to the default Baseline mixture. Although these training runs have not fully completed by the time of submission, it is reasonable to anticipate that they will eventually reach lower validation losses than the Baseline.
- Our **BIMIX**-optimized data mixture required only 40% of the total training steps (80,000 vs. 200,000) to achieve equivalent performance to the Baseline, significantly enhancing the learning efficiency from data. In contrast, while the data mixture of Ye et al. also demonstrated enhanced learning efficacy, it required as much as 85% of the training steps to achieve comparable performance.
- The efficacy of the data mixture driven by conditional entropy was only marginally eclipsed by the superior **BIMIX**, requiring 50% fewer training steps compared to the Baseline. Most importantly, this outcome was achieved without incurring any prior training overhead.

E Fitted Coefficients

Tables 8 and 7 present the fitted coefficient values for Equation 1 on the Pile and SlimPajama datasets, respectively. For ease of reference, we restate the proposed mixing law:

$$\mathcal{L}(s, r) = \left(\frac{\mathcal{A}}{s^\alpha} + \mathcal{C} \right) \frac{\mathcal{B}}{r^\beta},$$

The validation losses of SE, JE, CE, and VNE mixtures serve as the fitting observations. Note that the exponents α were fitted using training steps S scaled down by a factor of 10^4 .

Table 7: Fitted coefficients on the Pile dataset

Domain	\mathcal{A}	\mathcal{B}	\mathcal{C}	α	β
ArXiv	0.281	0.857	2.073	1.223	0.056
BookCorpus2	0.233	1.115	2.316	1.180	0.055
Books3	0.252	1.205	2.328	1.205	0.041
DM Mathematics	0.254	0.664	1.680	1.152	0.054
Enron Emails	0.440	0.853	1.548	0.996	0.114
EuroParl	0.345	1.122	1.481	1.170	0.076
FreeLaw	0.316	0.974	1.948	1.204	0.067
Github	0.352	0.735	1.512	1.176	0.082
Gutenberg (PG-19)	0.262	1.129	2.259	1.190	0.061
HackerNews	0.285	1.086	2.465	1.205	0.031
NIH ExPorter	0.244	1.092	1.971	1.221	0.075
OpenSubtitles	0.211	1.134	2.468	1.223	0.008
OpenWebText2	0.266	1.261	2.171	1.187	0.051
PhilPapers	0.271	1.222	2.194	1.123	0.049
Pile-CC	0.257	1.201	2.454	1.203	0.041
PubMed Abstracts	0.250	1.056	1.860	1.236	0.100
PubMed Central	0.224	1.113	1.639	1.232	0.080
StackExchange	0.272	0.954	1.859	1.211	0.077
USPTO Backgrounds	0.258	1.016	2.029	1.254	0.062
Ubuntu IRC	0.356	0.908	1.855	1.091	0.062
Wikipedia (en)	0.353	1.028	2.520	1.170	0.025
YoutubeSubtitles	0.520	0.674	2.533	1.142	0.054

Table 8: Fitted coefficients on the SlimPajama dataset

Domain	\mathcal{A}	\mathcal{B}	\mathcal{C}	α	β
ArXiv	0.245	0.988	1.654	1.201	0.055
Books	0.201	1.697	1.605	1.145	0.051
C4	0.209	1.607	1.785	1.132	0.075
CommonCrawl	0.257	1.415	2.023	1.145	0.048
Github	0.290	0.790	1.203	1.184	0.082
StackExchange	0.290	0.906	1.794	1.158	0.092
Wikipedia	0.340	1.260	1.565	1.111	0.070

F Mixture Recipes

Tables 9 and 10 present the refined data mixtures for the Pile and SlimPajama datasets, respectively. Here, ‘Default’ indicates the original composition of the datasets, ‘CE’ represents the proportions computed by conditional entropy, and ‘OPT’ refers to the optimized proportions using the proposed mixing law.

Table 9: Data mixtures on the Pile dataset

Domain	Default	CE	OPT
ArXiv	0.1207	0.0350	0.0507
BookCorpus2	0.0061	0.0461	0.0088
Books3	0.1013	0.0697	0.0392
DM Mathematics	0.0253	0.0078	0.0240
Enron Emails	0.0017	0.0272	0.0786
EuroParl	0.0103	0.0314	0.0648
FreeLaw	0.0491	0.0394	0.0441
GitHub	0.0580	0.0451	0.0812
Gutenberg (PG-19)	0.0307	0.0535	0.0373
HackerNews	0.0073	0.0474	0.0228
NIH ExPorter	0.0026	0.0406	0.0155
OpenSubtitles	0.0146	0.0202	0.0187
OpenWebText2	0.1064	0.0761	0.0443
PhilPapers	0.0043	0.0603	0.0372
Pile-CC	0.0947	0.0841	0.0423
PubMed Abstracts	0.0288	0.0497	0.0727
PubMed Central	0.1499	0.0462	0.0464
StackExchange	0.0660	0.0506	0.0616
USPTO Backgrounds	0.0339	0.0423	0.0387
Ubuntu IRC	0.0138	0.0281	0.0435
Wikipedia (en)	0.0649	0.0639	0.0789
YoutubeSubtitles	0.0095	0.0353	0.0486

Table 10: Data mixtures on the SlimPajama dataset

Domain	Default	CE	OPT
ArXiv	0.0458	0.0710	0.1266
Books	0.0420	0.1669	0.0264
C4	0.2660	0.2079	0.2620
CommonCrawl	0.5203	0.2175	0.1794
GitHub	0.0522	0.0902	0.1233
StackExchange	0.0337	0.1177	0.1497
Wikipedia	0.0399	0.1287	0.1325